## PAPER

# Synergistic interactions between multi-walled carbon nanotubes and toxic hexavalent chromium†

Hongbo Gu,[ab] Sowjanya B. Rapole,[ac] Yudong Huang,[b] Dongmei Cao,[d] Zhiping Luo,[e] Suying Wei[*c] and Zhanhu Guo[*a]

In this paper, the synergistic interactions between as-received multi-walled carbon nanotubes (MWNTs) and toxic hexavalent chromium (Cr(VI)) in solutions of different pH were investigated that aimed to functionalize the nanotubes and remove the toxic Cr(VI) by Fourier transform infrared spectroscopy (FT-IR), X-ray photoelectron spectroscopy (XPS), thermogravimetric analysis (TGA), Raman spectroscopy and transmission electron microscopy (TEM). The effects of pH value and MWNT concentration (dose) on Cr(VI) removal from polluted water with different initial Cr(VI) concentrations were investigated. Results revealed that MWNTs could be used for complete Cr(VI) removal through the reduction of Cr(VI) to Cr(III) in the polluted water with an initial Cr(VI) concentration ranging from 200 to 1000 µg L$^{-1}$ during half an hour treatment in a pH = 1.0 solution. The Cr(VI) solutions with different pH values had different effects on MWNTs. For pH = 1.0 Cr(VI) solution with a concentration of 1000 µg L$^{-1}$, the carboxyl and ether functional groups were found to form on the MWNT surface after 5 to 30 min Cr(VI) treatment and the carboxylate groups were formed as the treatment period increased to 60 min. The kinetics in different pH Cr(VI) solutions were derived. The redox kinetics in the pH = 1.0 solution was described by the pseudo-first-order behavior with respect to Cr(VI) and the typical value of the pseudo-first-order rate constant was calculated to be 0.05786 min$^{-1}$. In the pH = 7.0 solution, the adsorption kinetics rather than redox reaction dominated the Cr(VI) removal by the calculation and was explained by the pseudo-second-order model with a rate constant of 0.865 g mg$^{-1}$ min$^{-1}$.

## 1 Introduction

Hexavalent chromium (Cr(VI)) is a commonly identified contaminant in the groundwater arising from various industries including electroplating, leather tanning, cement, mining, and photography,[1–3] and can cause severe environmental and public health problems.[4] Cr(VI) is known to be detrimental to animals and humans and is carcinogenic.[5] Typically, in the acidic solutions, Cr(VI) has a very strong oxidative ability due to its high redox potential (1.33 V) and can be reduced to stable Cr(III) species.[6] The US Environmental Protection Agency (EPA) allows a maximum contaminant level (MCL) of 100 µg L$^{-1}$ for total chromium according to the national primary drinking water regulations.[7] Many treatment technologies have been reported to remove toxic Cr(VI), including cyanide treatment,[8] electro-chemical precipitation,[9] ion exchange, and adsorption.[10] Adsorption and Cr(VI) removal through chemical reduction from Cr(VI) to Cr(III) are the most versatile methods and are widely used for Cr(VI) removal.[6,11,12] Generally, Cr(III) hydroxo complexes are expected to be the dominating species of Cr(III) in natural waters.[13] Rai *et al.*[14] have described the precipitation/dissolution kinetics of Cr(OH)$_3$ and found that the data could be best described by a series of equilibriums involving three major monomeric solution species depending on the solution pH, *i.e.* CrOH$^{2+}$, Cr(OH)$_3$ and Cr(OH)$_4^-$. Normally, the solubility of Cr(OH)$_3$ between pH 6 and 10.5 is very low and the formation of a precipitate of Cr(OH)$_3$ is rapid. In the pH < 6 solution, CrOH$^{2+}$ is the dominating Cr species and in the pH > 12 solution, Cr(OH)$_4^-$ is the dominating Cr species. According to this observation, Cr(III) could be removed from the solution by adjusting the pH value of solution *via* a precipitation method in the case of regeneration of Cr(VI) in the solutions by the oxidation of Cr(III).[15]

Carbon nanotubes (CNTs) are an allotrope of carbon materials with graphene cylindrical nanostructures, mainly including single-walled carbon nanotubes (SWNTs) and

[a]*Integrated Composites Lab (ICL), Dan F. Smith Department of Chemical Engineering, Lamar University, Beaumont, TX 77710, USA. E-mail: zhanhu.guo@lamar.edu; Tel: +1 409 880 7654*

[b]*School of Chemical Engineering and Technology, Harbin Institute of Technology, Harbin 150001, Heilongjiang, China*

[c]*Department of Chemistry and Biochemistry, Lamar University, Beaumont, TX 77710, USA. E-mail: suying.wei@lamar.edu; Tel: +1 409 880 7976*

[d]*Material Characterization Center, Louisiana State University, LA 70803, USA*

[e]*Department of Chemistry and Physics and Southeastern North Carolina Regional Microanalytical and Imaging Consortium, Fayetteville State University, Fayetteville, NC 28301, USA*

† Electronic supplementary information (ESI) available. See DOI: 10.1039/c2ta00550f

This journal is © The Royal Society of Chemistry 2013

*J. Mater. Chem. A*, 2013, **1**, 2011–2021 | **2011**

multi-walled carbon nanotubes (MWNTs).[17] SWNTs only have a one-atom-thick layer of graphite (also called graphene), whereas MWNTs consist of multiple rolled layers of graphite.[18,19] Since the discovery of CNTs in 1991,[20] they have captured increasing attention due to their significantly large length-to-diameter ratio (132 000 000 : 1),[21] outstanding mechanical and electrical properties, as well as extraordinary thermal conductivity.[16,22] CNTs have been reported for their wide applications including hydrogen storage,[23] solar cells[24] and ultracapacitors.[25] Even though various available adsorbents like activated carbon,[8,26,27] sawdust,[28] cyanobacterium,[29] and bagasse fly ashes have been reported to remove hazardous heavy metals, most of these adsorbents have a low Cr(VI) adsorption capacity.[30] Compared with others, CNTs have been investigated as promising adsorbents for removing heavy metals and can be easily modified by chemical treatments to increase their adsorption capacity.[31] For example, chemical oxidation, carbonization processes, solvothermal methods, the arc-discharge technique and pyrolysis[32] have been used to prepare CNT-based functional materials such as magnetic CNT nanocomposites,[32] amino-functionalized CNTs[33] and acid-functionalized CNTs.[34] Though the Cr(VI) removal percentage and adsorption behaviors of these functionalized CNT materials from polluted water have been explored,[35,36] Cr(VI) removal by as-received CNTs was unfortunately rarely reported systemetically.[30] In addition, the synergistic interactions between the as-received CNTs and toxic Cr(VI) have been rarely explored. Understanding the surface functionalities of the CNTs will help the design of functional polymer nanocomposites, where the interfacial bonding and compatibility with the hosting polymer matrix is critically important.[16,19,37]

In this paper, the synergistic interactions between the as-received MWNTs and toxic Cr(VI) are explored under different conditions. The effects of the pH value, initial Cr(VI) concentration and MWNT concentration (dose) on these synergies have been studied. The surface functionalities of the MWNTs after treatment with Cr(VI) solutions having different pH values for different treatment times have been systematically studied using Fourier transform infrared spectroscopy (FT-IR), X-ray photoelectron spectroscopy (XPS), thermogravimetric analysis (TGA), Raman spectroscopy and transmission electron microscopy (TEM). The Cr(VI) removal percentage of the as-received MWNTs has been compared with that of the MWNTs oxidized by concentrated nitric acid. The kinetics of the as-received MWNTs in the Cr(VI) solutions with different pH values have also been investigated in detail.

## 2 Experimental

### 2.1 Materials

MWNTs (SW*e*NT SMW 200X, average diameter: 10.4 nm; average length: 4.3 μm) were provided by SouthWest Nano-Technologies, Inc. Potassium dichromate ($K_2Cr_2O_7$) and 1,5-diphenylcarbazide (DPC) were purchased from Alfa Aesar Company. Phosphoric acid ($H_3PO_4$, 85 wt%), acetone, nitric acid (68.0–70.0 wt%) and sulfuric acid (98 wt%) were obtained

from Fisher Scientific. All the chemicals were used as-received without any further treatment.

### 2.2 Preparation of oxidized MWNTs

MWNTs (1.0 g) were oxidized in 100 mL concentrated nitric acid (68.0–70.0 wt%) by mechanical stirring at 50 °C for one and half hours. After that, deionized water was used to wash the filtrate until the pH was about 7. Then the oxidized MWNTs obtained were dried in a vacuum oven at 80 °C overnight.

### 2.3 Synergistic interactions between Cr(VI) and MWNTs under different conditions

The potassium dichromate ($K_2Cr_2O_7$) stock solution (4.0 g $L^{-1}$) was prepared by dissolving potassium dichromate (1.1315 g) in 100.0 mL deionized water. The Cr(VI) standard solution was prepared by diluting 10.0, 12.5, 15.0, 17.5, 20.0, 25.0, 30.0, 37.5 μL potassium dichromate stock solution to 100.0 mL with deionized water. DPC solution was prepared by dissolving 50.0 mg DPC in 10.0 mL acetone (prepared freshly for each use). Phosphoric acid (4.5 M) was prepared by diluting 30.0 mL concentrated phosphoric acid (85.0% w/w) to 100.0 mL with deionized water.

The final Cr(VI) concentration was determined by the colorimetric method.[38] The obtained standard fitting curve was $A = 9.7232 \times 10^{-4} C$, where $C$ is the Cr(VI) concentration, $A$ is the absorbance obtained from the ultraviolet-visible spectroscopy (UV-vis, Cary 50) test,[39] from which the final Cr(VI) concentration of the solution was calculated.

The effect of pH on Cr(VI) removal was conducted by treating the as-received MWNTs with Cr(VI) solutions possessing pH values of 1.0, 2.0, 3.0, 5.0, 7.0, 9.0 and 11.0 at room temperature, respectively. The initial pH values of the Cr(VI) solutions were adjusted by 1.0 mol $L^{-1}$ NaOH and 1.0 mol $L^{-1}$ HCl with a pH meter (Vernier LabQuest with pH-BTA sensor). The pH = 1.0 Cr(VI) solution was adjusted by concentrated sulfuric acid (98 wt %). The MWNTs (20.0 mg) were ultrasonically (Branson 8510) dispersed in 20.0 mL solution with an initial Cr(VI) concentration of 1000.0 μg $L^{-1}$ over the same treatment period of 30 min. An appropriate amount of solution was taken out and centrifuged quickly (Fisher Scientific, Centrific 228). Then the supernatant (5.25 mL) was transferred into a test tube, in which the prepared $H_3PO_4$ solution (0.50 mL) and DPC solution (0.25 mL) were added. The mixed solution was incubated for 30 min for color development. Next, an appropriate portion of the above solution was transferred to a one cm cuvette for the UV-vis test.

To evaluate the degree of structural change of the MWNTs after treatment with pH = 1.0 Cr(VI) solution, the as-received MWNTs were treated with Cr(VI) solutions of 1000 μg $L^{-1}$ for a treatment period ranging from 5 to 60 min and treated with Cr(VI) solutions of 2 g $L^{-1}$ for a treatment period ranging from 5 to 30 min, respectively.

To investigate the effect of the initial Cr(VI) concentration on Cr(VI) removal, MWNTs (20.0 mg) were used to treat 20.0 mL pH = 1.0 Cr(VI) solutions with an initial Cr(VI) concentration varying from 400.0 to 1500.0 μg $L^{-1}$ for 30 min.

**2012** | *J. Mater. Chem. A*, 2013, **1**, 2011–2021

This journal is © The Royal Society of Chemistry 2013

The effects of MWNT concentration (dose) on Cr(VI) removal were investigated using various MWNT doses from 0.5 to 2.0 g $L^{-1}$ to treat 20.0 mL Cr(VI) solution with an initial Cr(VI) concentration of 1000.0 μg $L^{-1}$ at pH = 1.0 over the same treatment period of 30 min.

The kinetics of Cr(VI) removal by MWNTs from the pH = 1.0 and 7.0 solutions were investigated, respectively. Specifically, MWNTs (20.0 mg) were exposed to 20.0 mL pH = 1.0 Cr(VI) solution with an initial Cr(VI) concentration of 1000.0 μg $L^{-1}$ over different treatment periods from 5 to 25 min. For the pH = 7.0 solutions, the experiment was carried out according to the following procedure: MWNTs (20.0 mg) were exposed to 20.0 mL Cr(VI) neutral solutions with an initial Cr(VI) concentration of 600.0 μg $L^{-1}$ during different treatment times from 10 to 40 min. All the UV-vis absorption results are shown in the ESI;† the blank in the experiments means that the initial Cr(VI) concentration is 0.0 g $L^{-1}$.

The Cr(VI) removal percentage (R%) was calculated from eqn (1):

$$R\% = \frac{C_0 - C_e}{C_0} \times 100\% \quad (1)$$

where $C_0$ (mg $L^{-1}$) is the initial Cr(VI) concentration, and $C_e$ is the final Cr(VI) concentration of the solution after the treatment. All the Cr(VI) removal tests were carried out at room temperature.

## 2.4 Characterizations

The Fourier transform infrared spectroscopy (FT-IR) spectra of the products were obtained on a Bruker Inc. Vector 22 (coupled with an ATR accessory) in the range of 500 to 4000 $cm^{-1}$ at a resolution of 4 $cm^{-1}$.

The X-ray photoelectron spectroscopy (XPS) measurements were performed with a Kratos AXIS 165 XPS/AES instrument using monochromatic Al Kα radiation. The C1s peaks were deconvoluted into the components consisting of a Gaussian line shape Lorentzian function (Gaussian = 80%, Lorentzian = 20%) on a Shirley background.

Raman spectra were obtained using a Horiba Jobin-Yvon LabRam Raman confocal microscope with 785 nm laser excitation at a 1.5 $cm^{-1}$ resolution at room temperature. Thermogravimetric analysis (TGA) was conducted using a TA instruments Q-500 at a heating rate of 10 °C $min^{-1}$ and an air flow rate of 60 mL $min^{-1}$ from 25 to 800 °C.
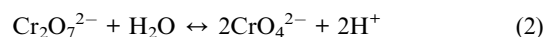
The morphology of the samples was characterized by a field emission transmission electron microscope (TEM, FEI Tecnai G2 F20), operated at an accelerating voltage of 200 kV. The samples were prepared by drying a drop of ethanol suspension on the carbon-coated copper TEM grids.

## 3 Results and discussion

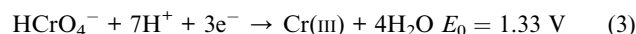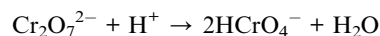### 3.1 Effect of Cr(VI) solutions on the carbon nanotubes

The solution pH is an important parameter influencing the Cr(VI) removal process. pH dependent heavy metal removal is related not only to the metal chemistry in the solution but also to the type of the adsorbents.[40,41] In the aqueous solution,

dichromate ions ($Cr_2O_7^{2-}$) are in equilibrium with chromate ions ($CrO_4^{2-}$), eqn (2):[42]

$$Cr_2O_7^{2-} + H_2O \leftrightarrow 2CrO_4^{2-} + 2H^+ \quad (2)$$

which is a dynamic equilibrium and is sensitive to the solution acidity. The equilibrium shifts by changing the pH value. When the solution is acidic, the equilibrium shifts to the left towards dichromate ions, which will spontaneously turn to $HCrO_4^-$ as the dominating species. However, for the basic solutions, the equilibrium shifts to the right and $CrO_4^{2-}$ is the only chromate in the solution.[42] Fig. 1a shows the Cr(VI) removal percentage from the solutions (20.0 mL) with different pH values after 30 min treatment with 20.0 mg MWNTs. The results demonstrate a pH dependent removal percentage. The Cr(VI) removal percentage is observed to decrease with increasing pH value from pH = 1.0 to 11.0. The Cr(VI) has been completely removed in the pH = 1.0 and 2.0 solutions. The Cr(VI) removal percentage is almost identical for the pH = 7.0 solution (30.0%) and for the pH = 9.0 solution (25.5%), no detectable Cr(VI) removal is observed in the pH = 11.0 solution. These results indicate that when pH > 7, Cr(VI) removal by the MWNTs is not efficient.

To better understand the synergistic interactions between the as-received MWNTs and Cr(VI) in the solutions with different pH values, the FT-IR spectra of the MWNTs treated with Cr(VI) solutions in different conditions were obtained, Fig. 2A. In the FT-IR spectrum of the as-received MWNTs, there is no obvious absorption peak observed, Fig. 2A-a, indicating very few functional groups on the surface of the as-received MWNTs.[37] In the FT-IR spectrum of the MWNT sample treated with pH = 1.0 Cr(VI) solution, Fig. 2A-c, the broad band at around 3300 $cm^{-1}$ corresponds to the O–H stretching from the carboxyl groups and the peak at 1641 $cm^{-1}$ is attributed to the C=O stretching. The peaks at around 1020–1100 $cm^{-1}$ are due to the C–O–C stretching. However, in the MWNT sample treated with concentrated nitric acid, Fig. 2A-b, only the peaks at 3300 and 1641 $cm^{-1}$ are observed without any visible peak at 1020–1100 $cm^{-1}$ for the C–O–C stretching. This indicates that the as-received MWNTs were functionalized with different functional groups after treatment with the pH = 1.0 Cr(VI) solution and concentrated nitric acid. Cr(VI) is known as a very strong oxidant due to its high redox potential, eqn (3), especially in pH < 2.0 acidic solutions:[43,44]

$$Cr_2O_7^{2-} + H^+ \rightarrow 2HCrO_4^- + H_2O$$

$$HCrO_4^- + 7H^+ + 3e^- \rightarrow Cr(III) + 4H_2O \quad E_0 = 1.33\ V \quad (3)$$

This means that a redox reaction occurred in the pH = 1.0 solutions, indicating that the MWNTs had been oxidized by Cr(VI) after treatment with Cr(VI) solution (pH = 1.0) and the C–O–C and carboxyl groups were formed on the MWNTs. However, in the pH > 2.0 solutions, the FT-IR spectra of the treated samples are almost the same as that of the as-received
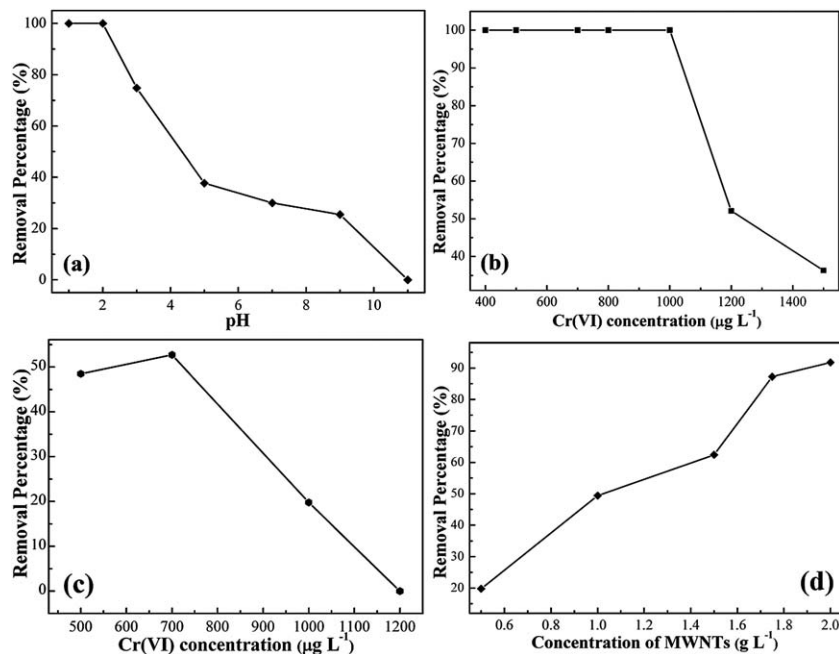
This journal is © The Royal Society of Chemistry 2013

*J. Mater. Chem. A*, 2013, **1**, 2011–2021 | **2013**

**Fig. 1** Cr(VI) removal percentage as a function of (a) pH value (20.0 mL 1000.0 μg L$^{-1}$ initial Cr(VI) concentration solution with 20.0 mg MWNTs after 30 min treatment); (b) initial Cr(VI) concentration (20.0 mL pH = 1.0 Cr(VI) solution, 20.0 mg as-received MWNTs and 30 min treatment); (c) initial Cr(VI) concentration (20.0 mL pH = 1.0 Cr(VI) solution, 20.0 mg oxidized MWNTs by nitric acid and 30.0 min treatment); (d) MWNT concentration (20.0 mL Cr(VI) pH = 1.0 solution with an initial Cr(VI) concentration of 1000.0 μg L$^{-1}$ after 30 min treatment).

MWNTs, Fig. 2A-b–f, indicating no functional groups formed in the MWNT samples treated with pH > 2.0 Cr(VI) solutions.

To further understand the interactions between MWNTs and Cr(VI) in the solutions with different pH values, TGA, XPS spectra and TEM microstructures of the as-received MWNTs and the MWNT samples treated with different pH solutions were obtained, Fig. 2B, 3 and 4. In the TGA curves, Fig. 2B, the as-received MWNTs exhibit only one-stage weight loss from 500 to 600 °C, which is due to the thermal degradation of the hexagonal carbon from the MWNTs.[45] The TGA curve of the MWNT sample treated with pH = 1.0 Cr(VI) solution has a different thermal degradation profile from that of others. Two-stage weight losses are observed in the MWNT sample treated with pH = 1.0 Cr(VI) solution. The first stage from room temperature to 200 °C is attributed to the degradation of the C–O–C groups,[46] which is verified by the FT-IR analysis, Fig. 2A-c. Then a plateau in the temperature range from 250 to 500 °C is observed. The second weight loss of the sample from 500 to 600 °C is due to the thermal degradation of the MWNTs. For all the other samples, the same thermal degradation processes are observed; however, they have different thermal stabilities. The degradation temperature (defined as a 5% weight loss) is 508, 463, 448, 480 and 480 °C for the as-received MWNT sample and the MWNT samples treated with pH = 3.0, 5.0, 7.0 and 9.0 Cr(VI) solutions, respectively. The MWNT samples treated with pH = 7.0 and 9.0 Cr(VI) solutions have the same degradation temperature. These results indicate that when pH is lower than 7.0, the Cr(VI) solution has a significant effect on the thermal stability of the treated MWNTs, but when pH > 7.0, the effect is not obvious.

Fig. 3a shows the XPS wide-scan survey spectra of the as-received MWNTs and the MWNTs treated with Cr(VI) solutions having different pH values. In the as-received MWNTs, only one main C1s binding energy peak at around 285 eV is observed. Compared with the as-received MWNTs, elemental oxygen has been observed on the surface of Cr(VI) treated MWNTs (the O1s binding energy peak at around 533 eV appears[47]), which arises mainly from the –COOH and C–O–C groups as verified by the FT-IR analysis of the MWNTs treated with pH = 1.0 Cr(VI) solution. Though the strong absorption peak related to the C–O–C group is not observed in the aforementioned FT-IR spectra of the MWNTs treated with pH = 5.0, 7.0 and 9.0 solutions (Fig. 2A-d–f), the observed O1s peak in the MWNT samples treated with pH = 5.0, 7.0 and 9.0 solutions, Fig. 3a, indicates some oxidation of the MWNTs after treated with Cr(VI) solutions at pH = 5.0, 7.0 and 9.0. The observed oxidation is not as strong as that of the MWNTs treated with pH = 1.0 solution, which is consistent with the decreased thermal stability observed in TGA.

Further analysis based on the deconvolution of the high resolution C1s XPS spectra of the as-received MWNTs and the MWNTs treated with pH = 1.0 Cr(VI) solution is conducted, Fig. 3b and c. The C1s peak of the as-received MWNTs is smoothly deconvoluted into three fitting curves with peaks at 284.9, 287.4 and 290.8 eV, corresponding to C=C, C=O and O–C=O, respectively, which are consistent with the previous report on the as-received MWNTs.[48] However, for the MWNT sample treated with pH = 1.0 Cr(VI) solution, a decreased C–C group peak intensity is observed and a new peak at around 286.1 eV appears, which is attributed to the C–O groups. Thus,
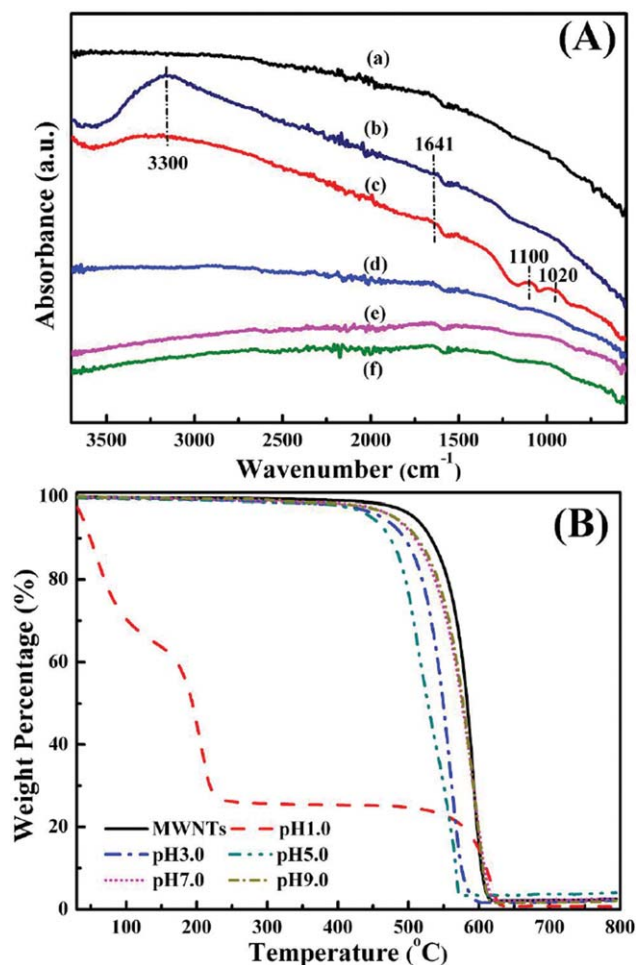
**Fig. 2** (A) FT-IR spectra of (a) the as-received MWNTs, (b) the MWNT sample treated with concentrated nitric acid, and the MWNT sample treated with 1000 μg L$^{-1}$ Cr(VI) solutions with a pH value of (c) 1.0, (d) 5.0, (e) 7.0, and (f) 9.0 for 30 min; (B) TGA curves of the as-received MWNTs and the MWNT samples after 30 min treatment with the Cr(VI) solutions with different pH values.

the C1s spectrum of the MWNTs treated with pH = 1.0 Cr(VI) solution is deconvoluted into four distinct curves and the peaks are located at the characteristic binding energies of 284.5, 286.1, 287.4 and 290.4 eV, respectively.[49] The presence of the peak at 286.1 eV for the MWNTs treated with pH = 1.0 Cr(VI) solution is consistent with the observation of the C–O group from the FT-IR analysis, Fig. 2A-c, indicating that the C–O groups exist on the MWNTs after treatment with pH = 1.0 Cr(VI) solution.

A high resolution XPS spectrum is used to confirm the Cr element valence state.[50] Generally, for the Cr2p XPS spectrum, the characteristic binding energy peaks at 577.0–578.0 eV and 586.0–588.0 eV correspond to Cr(III) and the characteristic binding energy peaks for the Cr(VI) are at 580.0–580.5 and 589.0–590.0 eV.[51] Fig. S5 in the ESI† shows the Cr2p spectra of the MWNTs (20 mg) after treatment with 100.0 mL pH = 1.0 Cr(VI) solution with a concentration of 2.0 g L$^{-1}$ for 20 min at room temperature. In the low Cr(VI) concentration solution, such as 1000 μg L$^{-1}$, the Cr element cannot be detected in the XPS spectra; thus a high Cr(VI) concentration of 2 g L$^{-1}$ is chosen for evaluating the Cr element valence state. The observed binding

energy peaks of Cr2p located at around 576.5 and 587.2 eV, characteristic of Cr(III),[51] confirm that the adsorbed Cr is in the Cr(III) form. The former arises from the Cr2p$_{3/2}$ orbital and the latter from the Cr2p$_{1/2}$ orbital.[52] The presence of Cr(III) implies that the Cr(VI) ions have been reduced to Cr(III) ions by the MWNTs in the pH = 1.0 solution.

Fig. 4 shows the TEM microstructures of the as-received MWNTs and the MWNTs treated with pH = 1.0 and 7.0 Cr(VI) solutions. The surface of the as-received MWNTs is very smooth, Fig. 4a, and the average diameter is about 10.4–11.2 nm, which is consistent with the information obtained from the company. However, after treatment with pH = 1.0 Cr(VI) solution, the surface becomes very rough and the average diameter is about 8.2 nm, Fig. 4b, indicating that the MWNTs have been highly etched. The surface and average diameter of the MWNT sample treated with pH = 7.0 Cr(VI) solution show no obvious change, Fig. 4c.

In order to evaluate the degree of surface structural change of the MWNTs in the course of interaction with Cr(VI), the MWNTs are treated with pH = 1.0 Cr(VI) solution (1000 μg L$^{-1}$) with a treatment period ranging from 5 to 60 min and by another Cr(VI) solution (2 g L$^{-1}$) with a treatment period ranging from 5 to 30 min. Generally, the Raman spectra are well known as an important way to obtain the structural characterization of graphitic materials, which can provide valuable information about the defects, stacking of the graphene layers and the crystallite size to the hexagonal axis,[53,54] which is normally not detectable in other analytical tools.[55] Fig. 5 shows the obtained Raman spectra. In the Raman spectra of the CNTs, the disorder-induced D-band at around 1300 cm$^{-1}$ indicates the presence of the defects on the nanotubes arising from the sp$^3$ C–C bonds formed in the surface treatment.[56] The tangential mode ($E_{2g}$ symmetry, graphite mode) G-band appearing at 1583 cm$^{-1}$ is due to the sp$^2$ C=C bond stretching vibrations.[57] In Fig. 5a, for the MWNT samples treated with 1000 μg L$^{-1}$ pH = 1.0 Cr(VI) solution, the intensity of D-band is found to be continuously increased, and the intensity of G-band is suppressed (slightly) with increasing treatment period from 5 to 60 min. The spectrum of the MWNT sample treated with 1000 μg L$^{-1}$ pH = 1.0 Cr(VI) solution for 5 min is shown in Fig. S6.† The increasing D band is generated by the preferentially formed oxygen species on the nanotube sidewalls.[57] The higher the intensity of D band, the more the number of oxygen species formed on the sidewalls of nanotubes, i.e. oxygen-related functional groups are introduced on the surface of the nanotubes by the 1000 μg L$^{-1}$ pH = 1.0 Cr(VI) treatment. This result is consistent with that obtained in XPS characterization (Fig. 3a and c, pH = 1.0, 30 min treated sample) and the functional groups include –COOH and –C–O–C– as verified by FT-IR, Fig. 2A-c. Especially for the 60 min treated sample, the G-band is almost disappeared, indicating that the MWNTs have been severely oxidized and the surface is covered by the oxygen-related functional groups. The new peak that has appeared at around 1430 cm$^{-1}$ is assigned to the stretching vibration of the carboxylate (O=C–O–) groups,[58,59] indicating that carboxylate groups are formed as the treatment period increases to 60 min. The formation of the carboxylate (O=C–O–) groups is further confirmed by FT-IR, Fig. S7.†
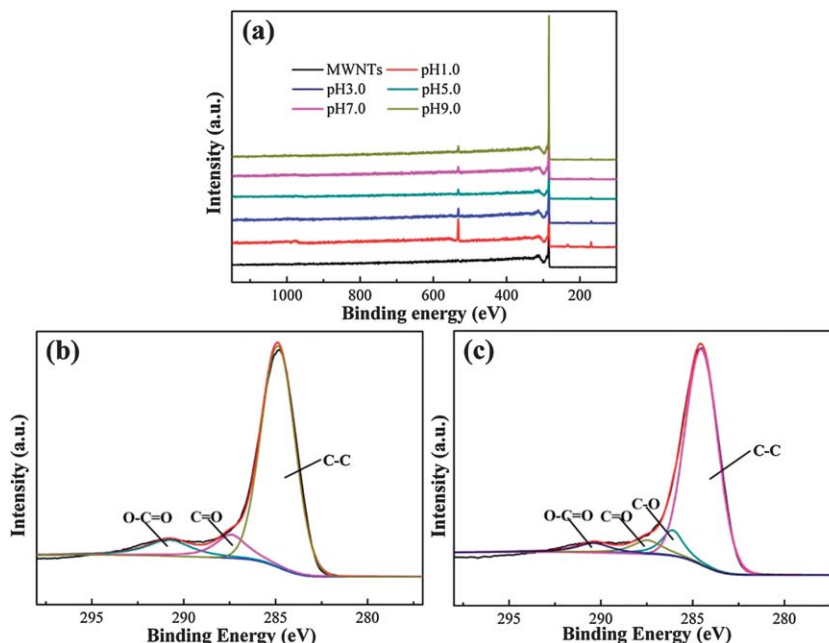
This journal is © The Royal Society of Chemistry 2013

*J. Mater. Chem. A*, 2013, **1**, 2011–2021 | **2015**

**Fig. 3** (a) XPS wide-scan survey spectra of the as-received MWNTs and the MWNT samples treated with 1000 µg L$^{-1}$ Cr(VI) solutions with different pH values for 30 min; deconvolution of high resolution C1s XPS spectra of (b) the as-received MWNTs and (c) the MWNTs treated with 1000 µg L$^{-1}$ Cr(VI) pH = 1.0 solution for 30 min.



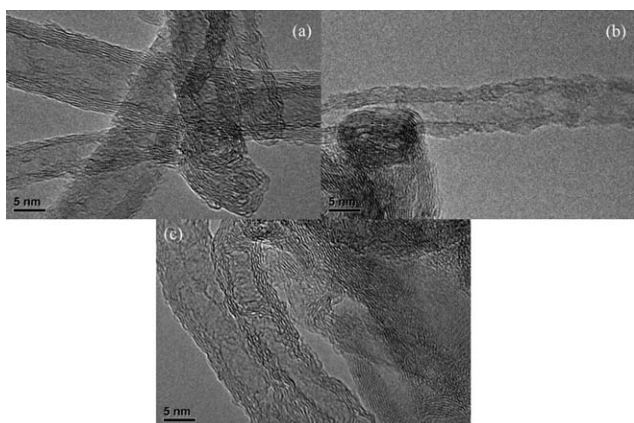**Fig. 4** TEM images of (a) the as-received MWNTs and the MWNT samples treated with 1000 µg L$^{-1}$ Cr(VI) solution with a pH of (b) 1.0 and (c) 7.0 for 30 min.

Interestingly, it is worth noting that the Cr(VI) concentration has a different effect on the treated MWNTs as well. In Fig. 5b, for the 2 g L$^{-1}$ pH = 1.0 Cr(VI) solution treated MWNT samples, the intensity of the D-band increases with increasing treatment time. However, the G-band only has a very weak signal after treatment with 2 g L$^{-1}$ pH = 1.0 Cr(VI) solution under 5 to 10 min and disappears as the treatment time increases to 20 min. A peak at around 1430 cm$^{-1}$ is observed, indicating that the carboxylate groups exist in all the treated samples and become obvious after a 20 min treatment. However, when the treatment period increases to 30 min, the peak at 1430 cm$^{-1}$ disappears and the G band appears again. The MWNTs have been severely oxidized by the Cr(VI) solution at high concentration with high oxidizing ability even for only 5 min treatment.

The TGA analysis is also used to investigate the structural change of the MWNTs treated with pH = 1.0 Cr(VI) solutions over different treatment periods ranging from 5 to 60 min and 5 to 30 min for initial Cr(VI) concentrations of 1000 µg L$^{-1}$ and 2 g L$^{-1}$, respectively. The results are shown in Fig. 6. In Fig. 6a, for the MWNT samples treated with 1000 µg L$^{-1}$ pH = 1.0 Cr(VI) solution, the weight loss from the degradation of the C–O–C groups at around 200 °C (ref. 46) increases with increasing treatment period from 5 to 30 min because the MWNT surfaces have attached oxygen functional groups as confirmed in the Raman analysis, Fig. 5. However, the MWNT sample treated with 1000 µg L$^{-1}$ Cr(VI) solution for 60 min has only a slight degradation at around 200 °C and the thermal stability is obviously improved compared with the as-received MWNTs, Fig. 6a. This is due to the more stable and complicated carboxylate groups formed, as justified by Raman (Fig. 5) and FT-IR (Fig. S6†) spectroscopy, arising from the chemical reaction between the attached –COOH and the –C–O–C– functional groups (Fig. 2A) on the MWNT sidewalls. In contrast, for the MWNT samples treated with 2 g L$^{-1}$ Cr(VI) solution, the thermal stability decreases as the treatment period increases to 20 min and then increases after 30 min treatment. However, the thermal stability of all the treated samples is lower than that of the as-received MWNTs. In addition, no obvious degradation of the C–O–C groups is observed in the MWNT samples treated with 2 g L$^{-1}$ Cr(VI) solution, which is due to the formation of the carboxylate groups as confirmed in the Raman test with the disappearance of the G band, Fig. 5b.

To summarize the effects of different pH Cr(VI) solutions, the initial Cr(VI) concentration and treatment period in pH = 1.0 Cr(VI) solution on the MWNTs from the above tests, the oxidation–reduction process between the MWNTs and Cr(VI) occurred

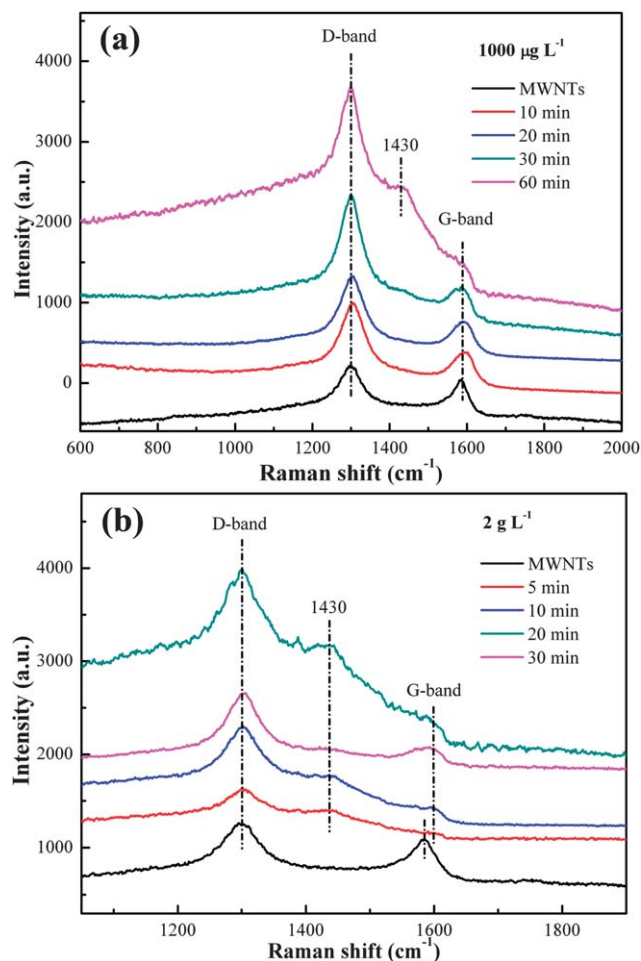**Fig. 5** Raman spectra of (a) the as-received MWNTs and the MWNT samples treated with 1000 µg $L^{-1}$ pH = 1.0 Cr(VI) solution with different treatment periods ranging from 10 to 60 min, and (b) the as-received MWNTs and the MWNT samples treated with 2 g $L^{-1}$ pH = 1.0 Cr(VI) solution with different treatment periods ranging from 5 to 60 min.



**Fig. 6** TGA curves of (a) the as-received MWNTs and the MWNT samples treated with 1000 µg $L^{-1}$ pH = 1.0 Cr(VI) solution with different treatment period ranging from 5 to 60 min, and (b) the as-received MWNTs and the MWNT samples treated with 2 g $L^{-1}$ pH = 1.0 Cr(VI) solution with different treatment periods ranging from 5 to 60 min.
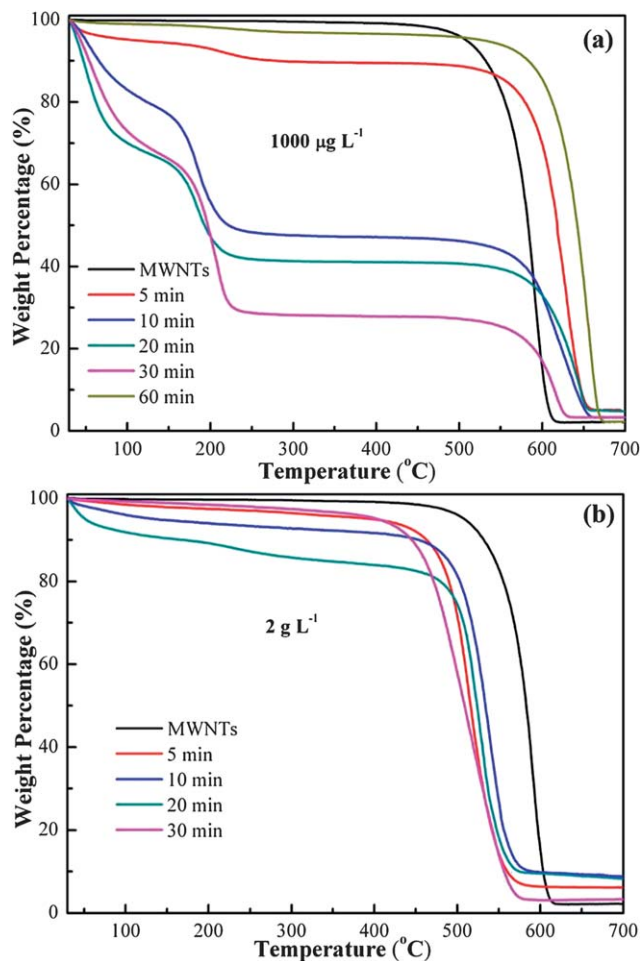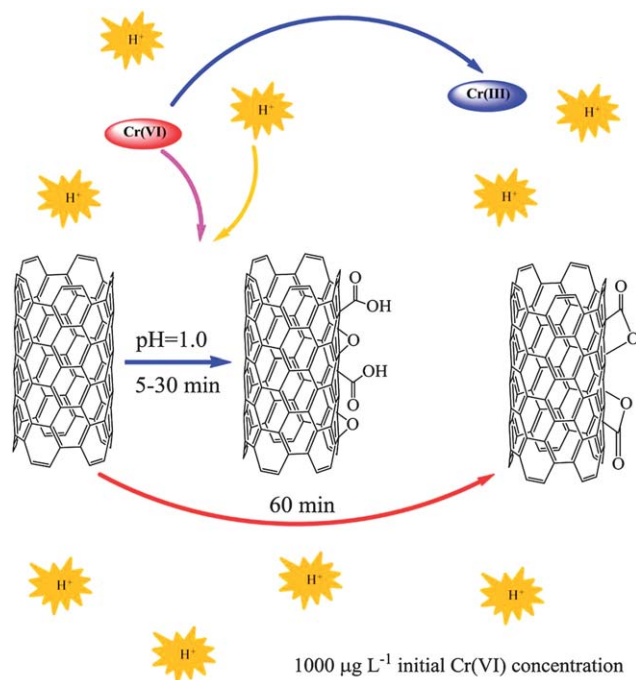
in the pH = 1.0 and 2.0 solutions; when pH > 2.0, the oxygen element is observed on the MWNTs in the XPS wide-scan survey spectra; however, the peak intensity is not as strong as that of the MWNTs treated with pH = 1.0 Cr(VI) solution. In the pH = 1.0 Cr(VI) solution with a concentration of 1000 µg $L^{-1}$, the COOH and –C–O–C– functional groups are formed on the MWNTs over a period from 5 to 30 min and the carboxylate groups are formed as the treatment period is increased to 60 min. The synergistic interaction between Cr(VI) and MWNTs in the pH = 1.0 solution with a Cr(VI) concentration of 1000 µg $L^{-1}$ is shown in Scheme 1.

## 3.2 Cr(VI) treatment by carbon nanotubes

Fig. 1b shows the effects of the initial Cr(VI) concentration on the Cr(VI) removal in the pH = 1.0 Cr(VI) solution over a treatment period of 30 min. The Cr(VI) is completely removed from the solutions with a Cr(VI) concentration ranging from 400.0 to 1000.0 µg $L^{-1}$, while only around 60% of the Cr(VI) is removed with increasing Cr(VI) concentration to 1200.0 µg $L^{-1}$. The

MWNTs have a very large specific surface area and large active sites for trapping the Cr(VI). However, these sites become saturated with increasing Cr(VI) concentration and cannot accommodate excessive Cr(VI) at higher Cr(VI) concentration.[60]

The MWNTs oxidized by concentrated nitric acid (20 mg) after treatment with Cr(VI) solutions (20.0 mL; pH = 1.0) of different initial Cr(VI) concentrations for the same treatment time were also investigated for comparison and the removal percentage is shown in Fig. 1c. Compared with Fig. 1b, the oxidized MWNTs exhibit a lower Cr(VI) removal percentage. The as-received MWNTs could remove the Cr(VI) from the solutions with an initial Cr(VI) concentration of 400.0–1000.0 µg $L^{-1}$ completely; however, the oxidized MWNTs only have 48.5, 52.7 and 19.8% removal percentages in the solutions with initial Cr(VI) concentrations of 500.0, 700.0, 1000.0 µg $L^{-1}$, respectively. The oxidized MWNTs have poor Cr(VI) removal performance for the solutions with an initial Cr(VI) concentration of 1200.0 µg $L^{-1}$, Fig. 1c. These results indicate that the as-received MWNTs have a better Cr(VI) removal performance than the concentrated nitric acid oxidized MWNTs.
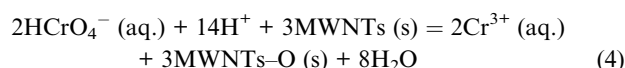
This journal is © The Royal Society of Chemistry 2013

*J. Mater. Chem. A*, 2013, **1**, 2011–2021 | **2017**

**Scheme 1** Reaction between the MWNTs and Cr(VI) in the pH = 1.0 Cr(VI) solution.

The effects of the MWNT concentration (dose) on the Cr(VI) removal percentage were tested over the same 30 min treatment, Fig. 1d. The removal percentage is observed to increase with increasing the MWNT concentration, which is due to the availability of more active sites for trapping Cr(VI).[61]

### 3.3 Cr(VI) treatment kinetics

The kinetics of Cr(VI) removal in the pH = 1.0 Cr(VI) solution was studied and the Cr(VI) concentration change during the treatment period is shown in Fig. S8.† The Cr(VI) concentration in the solution during a 25 min treatment period decreases from 1000.0 to 98.32 $\mu g\ L^{-1}$. The Cr(VI) has been completely removed over a 30 min treatment period, Fig. 1b. Regarding chemical reactions, they have different reaction orders and corresponding rate constants $k$. Typically, they can be called zero-, first-, second- and $n^{th}$-order reactions.[62] If the concentration of one or more kinetically active components is constant or nearly constant during the reaction process, the constant concentration will be included in the rate constant $k$ and the reaction is called "pseudo-$n^{th}$-order" reaction, and the rate constant is called pseudo-rate constant $k'$.[63]

The pseudo-first-order behavior has been reported for Cr(VI) reduction by polypyrrole,[64] polypyrrole-coated carbon substrate,[65] hydrogen peroxide,[66] iron[2,67] polyaniline film[68] and polyaniline–magnetite ($Fe_3O_4$) nanocomposites.[69] In order to obtain the kinetic plot of the Cr(VI) removal in the pH = 1.0 Cr(VI) solution, the pseudo-first-order kinetics is also introduced in this study. The reduction of the Cr(VI) by MWNTs is described by eqn (4):

$$2HCrO_4^- \text{ (aq.)} + 14H^+ + 3MWNTs \text{ (s)} = 2Cr^{3+} \text{ (aq.)} + 3MWNTs–O \text{ (s)} + 8H_2O \quad (4)$$

where MWNTs-O refers to the MWNTs after oxidized by Cr(VI). It is noticed that the reaction rate is related to three different species: $HCrO_4^-$, $H^+$ and MWNTs. Accordingly, the rate equation for the chemical reaction is mathematically expressed as, eqn (5):[68]
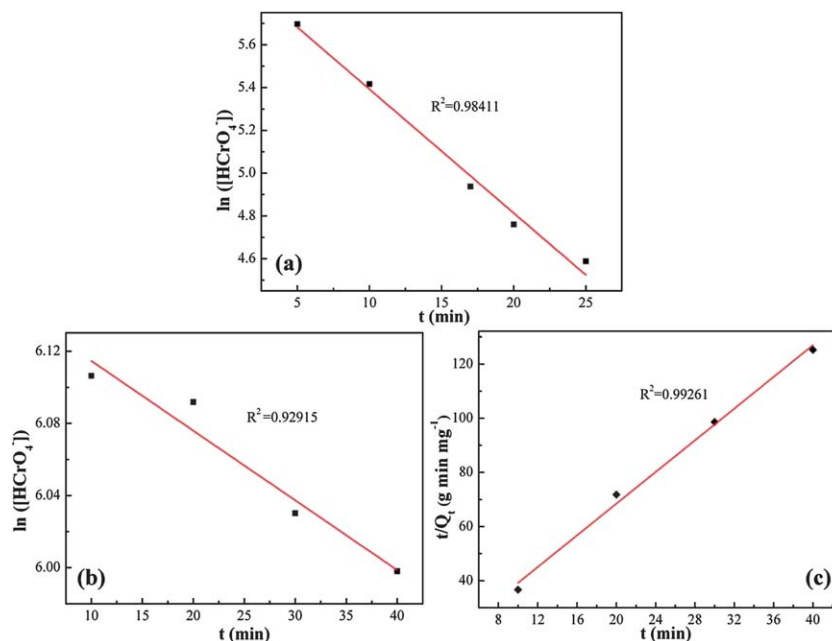


**Fig. 7** Kinetic plots of (a) $\ln([HCrO_4^-])$ vs. $t$ (Cr(VI) concentration: 1000.0 $\mu g\ L^{-1}$, 20.0 mL, pH = 1.0, MWNTs: 20.0 mg); (b) $\ln([HCrO_4^-])$ vs. $t$ (Cr(VI) concentration: 600.0 $\mu g\ L^{-1}$, 20.0 mL, pH = 7.0, MWNTs: 20.0 mg); (c) $t/Q_t$ vs. $t$ (Cr(VI) concentration: 600.0 $\mu g\ L^{-1}$, 20.0 mL, pH = 7.0, MWNTs: 20.0 mg) at room temperature.

**2018** | *J. Mater. Chem. A*, 2013, **1**, 2011–2021

This journal is © The Royal Society of Chemistry 2013

$$v = \frac{d[Cr(VI)]}{dt} = -k\left[HCrO_4^-\right]^m[MWNTs]^n[H^+]^p \quad (5)$$

where $k$ is the rate constant, the exponents ($m$, $n$ and $p$) are called reaction orders, which depend on the reaction mechanism; and $[HCrO_4^-]$, $[MWNTs]$ and $[H^+]$ are the concentrations of $HCrO_4^-$, MWNTs, $H^+$ at any given time, respectively. However, since $H^+$ is normally used as catalysts in this reaction[63] and MWNTs are solid and their concentration is much higher than $[HCrO_4^-]$, $[HCrO_4^-]$ is the most important factor to determine the reaction rate, and the rate equation (5) is written by eqn (6).

$$v = \frac{d[Cr(VI)]}{dt} = -k'\left[HCrO_4^-\right]^1 \quad (6)$$

where $k'$ stands for a pseudo-first-order rate constant. The representative kinetic plot for this study obtained from Fig. S8-b† and eqn (6) is shown in Fig. 7a. The observed linear relation between $\ln([HCrO_4^-])$ and $t$ with a fitting correlation coefficient $R^2$ of 0.98411 indicates a pseudo-first-order reaction between Cr(VI) and MWNTs. The typical value for the pseudo-first-order rate constant obtained from the slope is 0.05786 min$^{-1}$.

The kinetics of the Cr(VI) removal in the pH = 7.0 solution is also investigated using both eqn (6) (chemical reaction kinetics) and S4† (adsorption kinetics). Fig. S9† shows the Cr(VI) concentration change *vs.* the treatment time (Fig. S9-b†) and the obtained Cr(VI) removal rate $Q_t$ *vs.* time $t$ in pH = 7.0 solution, Fig. S9-c.† The representative kinetic plots obtained from Fig. S9-b and c† are shown in Fig. 7b and c. The fitting correlation coefficient $R^2$ values are 0.92915 and 0.99261, respectively. This indicates that the MWNTs follow more adsorption rather than redox reaction during the Cr(VI) removal in the pH = 7.0 solution. The kinetics of the Cr(VI) removal with the MWNTs in the pH = 7.0 solution follows a pseudo-second-order behavior in this study (refer to ESI,† adsorption kinetics). The slope and the intercept obtained from the plot (Fig. 7c) are 2.9278 and 9.905, respectively. The $Q_e$, $k_2$ and $h$ calculated according to the eqn (S4) and (S5)† are 0.342 mg g$^{-1}$, 0.865 g mg$^{-1}$ min$^{-1}$ and 0.101 mg g$^{-1}$ min$^{-1}$, respectively. This material shows a higher rate constant of 0.865 g mg$^{-1}$ min$^{-1}$ than that (0.28 g mg$^{-1}$ min$^{-1}$) of the magnetic graphene nanocomposite materials.[39]

## 4 Conclusions

In this paper, the synergistic interactions between the multi-walled carbon nanotubes (MWNTs) and the toxic Cr(VI) solutions with different pH values were investigated. FT-IR, TGA, XPS and TEM analyses show that Cr(VI) in the solutions with different pH values has different effects on the MWNTs. For the pH = 1.0 Cr(VI) solution, the as-received MWNTs are strongly oxidized by Cr(VI) and could be used for complete Cr(VI) removal through the reduction of Cr(VI) to Cr(III) from pH = 1.0 solutions with an initial Cr(VI) concentration from 200.0 to 1000.0 μg L$^{-1}$ over half an hour treatment. In the pH = 1.0 Cr(VI) solution with a concentration of 1000 μg L$^{-1}$, the COOH and C–O–C functional groups are formed on the MWNTs over a period from 5 to 30 min and the carboxylate groups are formed as the treatment period increases to 60 min.

For the pH > 2.0 solutions, the Cr(VI) removal percentage decreases dramatically and some oxidation of the MWNTs is also observed, which is not as intensive as that in the pH = 1.0 solution. The kinetics for different Cr(VI) removal mechanisms shows that in the pH = 1.0 solution, the redox kinetics dominates the Cr(VI) removal process and follows a pseudo-first-order behavior with respect to Cr(VI) concentration and the obtained typical value for the pseudo-first-order rate constant is 0.05786 min$^{-1}$. However, in the pH = 7.0 solution, the adsorption kinetics rather than redox reaction dominates by the calculation and is explained by a pseudo-second-order model with a rate constant of 0.865 g mg$^{-1}$ min$^{-1}$. These synergistic interaction investigations favor the applications of the carbon nanotubes with tailored surface functional groups for preparing multifunctional polymer nanocomposites such as the polyaniline stabilized carbon nanotubes reinforced epoxy nanocomposites[37] and potential electrochemical energy storage.[70]

## References

1 A. A. Hasin, S. J. Gurman, L. M. Murphy, A. Perry, T. J. Smith and P. H. E. Gardiner, *Environ. Sci. Technol.*, 2009, **44**, 400–405.

2 R. M. Powell, R. W. Puls, S. K. Hightower and D. A. Sabatini, *Environ. Sci. Technol.*, 1995, **29**, 1913–1922.

3 M. Bhaumik, A. Maity, V. V. Srinivasu and M. S. Onyango, *J. Hazard. Mater.*, 2011, **190**, 381–390.

4 L. A. M. Ruotolo and J. C. Gubulin, *Chem. Eng. J.*, 2009, **149**, 334–339.

5 K. M. Sirk, N. B. Saleh, T. Phenrat, H. J. Kim, B. Dufour, J. Ok, P. L. Golas, K. Matyjaszewski, G. V. Lowry and R. D. Tilton, *Environ. Sci. Technol.*, 2009, **43**, 3803–3808.

6 P. A. Kumar and S. Chakraborty, *J. Hazard. Mater.*, 2009, **162**, 1086–1098.

7 D. Zhang, S. Wei, C. Kaila, X. Su, J. Wu, A. B. Karki, D. P. Young and Z. Guo, *Nanoscale*, 2010, **2**, 917–919.

8 L. Monser and N. Adhoum, *Sep. Purif. Technol.*, 2002, **26**, 137–146.

9 N. Kongsricharoern and C. Polprasert, *Water Sci. Technol.*, 1995, **31**, 109–117.

10 Y. C. Sharma, B. Singh, A. Agrawal and C. H. Weng, *J. Hazard. Mater.*, 2008, **151**, 789–793.

11 H. Cui, M. Fu, S. Yu and M. K. Wang, *J. Hazard. Mater.*, 2011, **186**, 1625–1631.

12 J. Zhu, H. Gu, S. B. Rapole, Z. Luo, S. Pallavkar, N. Haldolaarachchige, T. J. Benson, T. C. Ho, J. Hopper, D. P. Young, S. Wei and Z. Guo, *RSC Adv.*, 2012, **2**, 4844–4856.

13 L. Spiccia, *Inorg. Chem.*, 1988, **27**, 432–434.

This journal is © The Royal Society of Chemistry 2013

*J. Mater. Chem. A*, 2013, **1**, 2011–2021 | **2019**

14 D. Rai, B. M. Sass and D. A. Moore, *Inorg. Chem.*, 1987, **26**, 345–349.

15 A. D. Apte, S. Verma, V. Tare and P. Bose, *J. Hazard. Mater.*, 2005, **121**, 215–222.

16 J. Zhu, X. Zhang, N. Haldolaarachchige, Q. Wang, Z. Luo, J. Ryu, D. P. Young, S. Wei and Z. Guo, *J. Mater. Chem.*, 2012, **22**, 4996–5005.

17 X. Wang, J. Lu and B. Xing, *Environ. Sci. Technol.*, 2008, **42**, 3207–3212.

18 H. Khani, M. K. Rofouei, P. Arab, V. K. Gupta and Z. Vafaei, *J. Hazard. Mater.*, 2010, **183**, 402–409.

19 J. Zhu, H. Gu, Z. Luo, N. Haldolaarachige, D. P. Young, S. Wei and Z. Guo, *Langmuir*, 2012, **28**, 10246–10255.

20 S. Iijima, *Nature*, 1991, **354**, 56–58.

21 X. Wang, Q. Li, J. Xie, Z. Jin, J. Wang, Y. Li, K. Jiang and S. Fan, *Nano Lett.*, 2009, **9**, 3137–3141.

22 M. F. Yu, B. S. Files, S. Arepalli and R. S. Ruoff, *Phys. Rev. Lett.*, 2000, **84**, 5552–5555.

23 A. C. Dillon, K. M. Jones, T. A. Bekkedahl, C. H. Kiang, D. S. Bethune and M. J. Heben, *Nature*, 1997, **386**, 377–379.

24 D. M. Guldi, G. M. A. Rahman, M. Prato, N. Jux, S. Qin and W. Ford, *Angew. Chem.*, 2005, **117**, 2051–2054.

25 H. Pan, J. Li and Y. Feng, *Nanoscale Res. Lett.*, 2010, **5**, 654–668.

26 D. Mohan, K. P. Singh and V. K. Singh, *J. Hazard. Mater.*, 2008, **152**, 1045–1053.

27 M. A. A. Zaini, R. Okayama and M. Machida, *J. Hazard. Mater.*, 2009, **170**, 1119–1124.

28 M. Uysal and I. Ar, *J. Hazard. Mater.*, 2007, **149**, 482–491.

29 V. K. Gupta and A. Rastogi, *J. Hazard. Mater.*, 2008, **154**, 347–354.

30 V. K. Gupta, S. Agarwal and T. A. Saleh, *Water Res.*, 2011, **45**, 2207–2212.

31 C. L. Chen, X. K. Wang and M. Nagatsu, *Environ. Sci. Technol.*, 2009, **43**, 2362–2367.

32 Z. Sun, Z. Liu, Y. Wang, B. Han, J. Du and J. Zhang, *J. Mater. Chem.*, 2005, **15**, 4497–4501.

33 W. Li, C. Gao, H. Qian, J. Ren and D. Yan, *J. Mater. Chem.*, 2006, **16**, 1852–1859.

34 G.-X. Chen, H.-S. Kim, B. H. Park and J.-S. Yoon, *J. Phys. Chem. B*, 2005, **109**, 22237–22243.

35 X. Lv, J. Xu, G. Jiang and X. Xu, *Chemosphere*, 2011, **85**, 1204–1209.

36 J. Wang, X. Ma, G. Fang, M. Pan, X. Ye and S. Wang, *J. Hazard. Mater.*, 2011, **186**, 1985–1992.

37 H. Gu, S. Tadakamalla, X. Zhang, Y.-D. Huang, Y. Jiang, H. A. Colorado, Z. Luo, S. Wei and Z. Guo, *J. Mater. Chem. C*, 2013, DOI: 10.1039/c1032tc00379a.

38 M. Gardner and S. Comber, *Analyst*, 2002, **127**, 153–156.

39 J. Zhu, S. Wei, H. Gu, S. B. Rapole, Q. Wang, Z. Luo, N. Haldolaarachchige, D. P. Young and Z. Guo, *Environ. Sci. Technol.*, 2012, **46**, 977–985.

40 S. Mor, K. Ravindra and N. R. Bishnoi, *Bioresour. Technol.*, 2007, **98**, 954–957.

41 V. K. Gupta, A. K. Shrivastava and N. Jain, *Water Res.*, 2001, **35**, 4079–4085.

42 Y. Li, B. Gao, T. Wu, D. Sun, X. Li, B. Wang and F. Lu, *Water Res.*, 2009, **43**, 3067–3075.

43 P. A. Kumar, S. Chakraborty and M. Ray, *Chem. Eng. J.*, 2008, **141**, 130–140.

44 R. Ansari, *Chin. J. Chem.*, 2006, **53**, 88–94.

45 A. C. Baudouin, J. Devaux and C. Bailly, *Polymer*, 2010, **51**, 1341–1354.

46 G. C. M. Santander, G. R. M. Sandra, N. de L. da Silva, de C. L. Camargo, T. G. Kieckbusch and M. R. W. Maciel, *Fuel*, 2012, **92**, 158–161.

47 L. Shao, Y. P. Bai, X. Huang, L. H. Meng and J. Ma, *J. Appl. Polym. Sci.*, 2009, **113**, 1879–1886.

48 T. Xu, J. Yang, J. Liu and Q. Fu, *Appl. Surf. Sci.*, 2007, **253**, 8945–8951.

49 T. I. T. Okpalugo, P. Papakonstantinou, H. Murphy, J. McLaughlin and N. M. D. Brown, *Carbon*, 2005, **43**, 153–161.

50 C.-Y. Lee, G. M. Harbers, D. W. Grainger, L. J. Gamble and D. G. Castner, *J. Am. Chem. Soc.*, 2007, **129**, 9429–9438.

51 D. Park, Y. S. Yun and J. M. Park, *J. Colloid Interface Sci.*, 2008, **317**, 54–61.

52 B. A. Manning, J. R. Kiser, H. Kwon and S. R. Kanel, *Environ. Sci. Technol.*, 2006, **41**, 586–592.

53 M. A. Pimenta, G. Dresselhaus, M. S. Dresselhaus, L. G. Cancado, A. Jorio and R. Saito, *Phys. Chem. Chem. Phys.*, 2007, **9**, 1276–1290.

54 L. G. Cançado, K. Takai, T. Enoki, M. Endo, Y. A. Kim, H. Mizusaki, A. Jorio, L. N. Coelho, R. Magalhães-Paniago and M. A. Pimenta, *Appl. Phys. Lett.*, 2006, **88**, 163106.

55 M. S. Dresselhaus and P. C. Eklund, *Adv. Phys.*, 2000, **49**, 705–814.

56 D. McIntosh, V. N. Khabashesku and E. V. Barrera, *J. Phys. Chem. C*, 2007, **111**, 1592–1600.

57 Y. C. Jung, H. H. Kim, Y. A. Kim, J. H. Kim, J. W. Cho, M. Endo and M. S. Dresselhaus, *Macromolecules*, 2010, **43**, 6106–6112.

58 S. J. Lee and M. Moskovits, *Nano Lett.*, 2011, **11**, 145–150.

59 T. Schmid, A. Messmer, B.-S. Yeo, W. Zhang and R. Zenobi, *Anal. Bioanal. Chem.*, 2008, **391**, 1907–1916.

60 K. Pillay, E. M. Cukrowska and N. J. Coville, *J. Hazard. Mater.*, 2009, **166**, 1067–1075.

61 J. Hu, C. Chen, X. Zhu and X. Wang, *J. Hazard. Mater.*, 2009, **162**, 1542–1550.

62 J. M. Coulson, J. F. Richardson and D. G. Peacock, in *Coulson & Richardson's Chemical Engineering: Chemical and Biochemical Reactors and Process Control (3rd edn, 2003)*, ed. D. G. Peacock, Elsevier, 1994, pp. 15–17.

63 J. W. Moore, R. G. Pearson and A. A. Frost, *Kinetics and mechanism*, Wiley, 1961.

64 R. Senthurchelvan, Y. Wang, S. Basak and K. Rajeshwar, *J. Electrochem. Soc.*, 1996, **143**, 44–51.

65 F. J. Rodríguez, S. Gutiérrez, J. G. Ibanez, J. L. Bravo and N. Batina, *Environ. Sci. Technol.*, 2000, **34**, 2018–2023.

**2020** | *J. Mater. Chem. A*, 2013, **1**, 2011–2021

This journal is © The Royal Society of Chemistry 2013

66 M. Pettine, L. Campanella and F. J. Millero, *Environ. Sci. Technol.*, 2002, **36**, 901–907.

67 M. J. Alowitz and M. M. Scherer, *Environ. Sci. Technol.*, 2002, **36**, 299–306.

68 S. T. Farrell and C. B. Breslin, *Environ. Sci. Technol.*, 2004, **38**, 4671–4676.

69 H. Gu, S. Rapole, J. Sharma, Y. Huang, D. Cao, H. A. Colorado, Z. Luo, N. Haldolaarachchige, D. P. Young, S. Wei and Z. Guo, *RSC Adv.*, 2012, **2**, 11007–11018.

70 J. Shen, A. Liu, Y. Tu, G. Foo, C. Yeo, M. Chan-Park, R. Jiang and Y. Chen, *Energy Environ. Sci.*, 2011, **4**, 4220–4229.

This journal is © The Royal Society of Chemistry 2013

*J. Mater. Chem. A*, 2013, **1**, 2011–2021 | **2021**